

# Trapped-Particle-Mediated Collisional Damping of Non-Axisymmetric Plasma Waves

Andrey A. Kabantsev and C. Fred Driscoll

*Department of Physics, University of California at San Diego, La Jolla, California 92093*

**Abstract.** Weak axial ripples in magnetic or electric confinement fields in pure electron plasmas cause slow electrons to be trapped locally, and collisional diffusion across the trapping separatrix then causes surprisingly large trapped-particle-mediated (TPM) damping and transport effects. Here, we characterize TPM damping of  $m_\theta \neq 0$ ,  $m_z = \pm 1$  Trivelpiece-Gould (TG) plasma modes in large amplitude long-lived BGK states. The TPM damping gives  $\gamma_{\text{BGK}}/\omega \sim 10^{-4}$ , and seems to dominate in regimes of weak collisions.

**Keywords:** BGK modes, nonneutral plasmas, magnetic ripples, separatrix

**PACS:** 52.27.Gt; 52.35.fp; 52.35.Sb

In typical pure electron plasma columns, the magnetic field is axially “invariant” to within 1 part in  $10^3$ ; but the slow electrons trapped in the weak ripples are predicted to have near-discontinuous velocity distributions, and this apparently causes dominant damping and transport effects. These trapped-particle-mediated (TPM) effects arise from both magnetic and electric ripples, and have been observed to cause new modes [1], damping of drift modes [2], cross-field transport of particles [2, 3, 4], as well as the damping of electron plasma waves discussed here. Theory suggests that TPM effects dominate when collision rates  $\nu$  are small compared to wave frequencies  $\omega$ , since TPM effects are predicted to scale as  $(\nu/\omega)^{1/2}$  rather than as  $(\nu/\omega)^1$ .

Of course, magnetic and electric trapping is commonplace in neutral plasma physics. In toroidal geometry, the enhanced inboard magnetic field strongly constrains the poloidal rotation, and gives rise to a variety of trapped particle modes and induced currents. An incisive boundary layer analysis of the trapping separatrix predicted near-discontinuous distribution functions, with damping effects scaling as  $(\nu/\omega)^{1/2}$  [5]. Later experimental work verified some aspects of trapped particle modes (but not the damping) [6, 7]. Only a few theorists have tackled the subtle  $(\nu/\omega)^{1/2}$  trapping scaling [8]. In stellarator magnetic fields a variety of TPM effects are thought to arise from helical ripples [9], but experimental tests are difficult.

In contrast, theory and experiment are in general accord on a variety of phase-space *wave-trapping* effects. Particles moving near the wave phase velocity can be trapped in the wave potential, causing a localized flattening of the (presumed) Maxwellian distribution, voiding Landau damping, and enabling “steady-state” Bernstein-Greene-Kruskal (BGK) modes [10]. For electron plasma waves, the initial wave amplitude exhibits oscillations that correspond closely to theory [11], and a variety of long-lived BGK states have been observed, including many with nonlinear frequency shifts [12, 13]. The recently-studied Electron Acoustic Waves exist only as nonlinear BGK states [14].

Surprisingly, the requisite wave-particle correlations persist even for standing waves in finite length apparatuses, surviving  $10^3$ – $10^4$  end reflections of oppositely moving waves. In the present experiments, the BGK state flattens the  $\pm\hat{z}$  velocity distribution for a 0.5% component of electrons, over the range  $0 < |v| < 5\bar{v}$ .

Velocity-scattering collisions necessarily dissipate these BGK states. Zakharov and Karpman [15] and others [16, 17] calculated repopulation of the Maxwellian distribution at the wave phase velocity, predicting damping rates  $\gamma_{\text{ZK}} \propto v^1$ .

In this paper, we observe a stronger damping of linear and large-amplitude waves, determined to be due to TPM effects, with damping rates consistent with a  $(v/\omega)^{1/2}$  scaling. The trapping arises from an inherent magnetic ripple with peak  $\delta B_z/B_z \sim 10^{-3}$  centered under the mid-plane cylinder, and from negative “squeeze” voltages intentionally applied to that cylinder. This TPM damping is observed only for  $m_\theta \neq 0$  modes, in which  $\hat{\theta}$  electric fields cause radial particle drifts, with consequent phase-space discontinuities at the ripple-trapping separatrix. Analogous TPM effects would be expected in neutral plasmas.

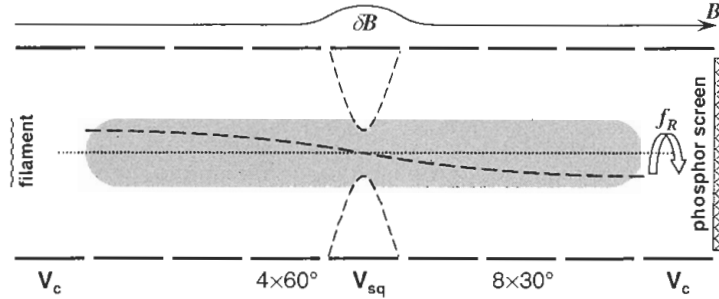


**FIGURE 1.** Schematic of cyclinridal electron plasma with magnetic and electric ripples, and an  $m_z = 1$  plasma wave.

The pure electron plasma columns described here are confined in a Penning-Malmberg trap, as shown in Fig. 1. The electrons emitted from a hot tungsten source are confined radially by a nearly uniform axial magnetic field  $1 \leq B \leq 15$  kG, and confined axially by negative voltages  $V_c = -100$  V on end cylinders with radius  $R_w = 3.5$  cm. Typical electron columns have density  $n \sim 1.5 \times 10^7$  cm $^{-3}$  over a radius  $R_p \sim 1.2$  cm and length  $L_p \sim 48$  cm, giving line density  $N_L \equiv \pi R_p^2 n_0 = 6.7 \times 10^7$  cm $^{-1}$ . The unneutralized electron charge results in an  $\mathbf{E} \times \mathbf{B}$  rotation of the column at frequency  $f_R(r) \sim 0.1$  MHz  $(B/2 \text{ kG})^{-1}$ .

The  $z$ -averaged densities  $\bar{n}(r, \theta, t)$  are measured at any time by dumping the electrons axially onto a phosphor screen imaged by a CCD camera. Alternately, the  $z$ -averaged density of the right-hand end *only*,  $\bar{n}_h(r, \theta, t)$ , can be measured by cutting the plasma in half with  $V_{\text{sq}} \sim -100$  V immediately ( $0.2 \mu\text{s}$ ) before dumping onto the phosphor. Additionally, the distribution of axial energies  $F(E_z)$  can be obtained by measuring the electrons which escape (preferentially near  $r = 0$ ) as the end confinement  $V_c$  is slowly raised to ground (in  $100 \mu\text{s}$ ). The initial quiescent plasmas have a thermal distribution with  $T \sim 1$  eV, giving  $\bar{v} \sim 42$  cm/ $\mu\text{s}$ ,  $\lambda_D \sim 0.2$  cm, and collisional  $90^\circ$  scattering rate  $\nu_{ee} \sim 160$  sec $^{-1}$ .

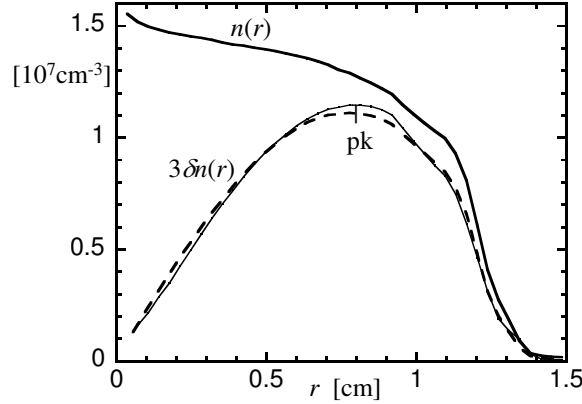


**FIGURE 2.** Measured plasma density  $n(r)$  and radial eigenfunction  $\delta n(r)$  of the  $m_\theta = 1, m_z = 1, m_r = 1$  plasma wave. The dashed line shows Eq. (3).

Electron-plasma waves in the Trivelpiece-Gould (TG) regime are excited and monitored on two cylinders with  $4 \times 60^\circ$  and  $8 \times 30^\circ$  wall sectors, allowing unambiguous identification of the axial and azimuthal mode numbers  $m_z$  and  $m_\theta$ . The modes are weakly damped standing waves in  $z$ , and have the form

$$\delta n(r, \theta, z, t) = \delta n(r) \sin(m_z \pi z / L_p) \cos[m_\theta \theta - 2\pi f t] e^{-\gamma t}. \quad (1)$$

Here, we focus on  $m_z = 1, m_\theta = 1$ , in the lowest radial mode ( $m_r = 1$ ) with  $\delta n(r) = 0$  only at  $r = 0$  and  $r > R_p$ .

Two separate TG modes exist at each  $m_\theta \neq 0$ , either co- or counter-rotating relative to the plasma  $f_R$ . The linearized cold electron plasma dispersion relation for top-hat density profiles predicts (upper, lower) frequencies

$$\begin{aligned} f_{u,\ell} &= m_\theta f_R \pm f_* \\ &\equiv m_\theta f_R \pm m_z \left( \frac{\pi R_p}{j_{m_\theta-1, m_r} L_p} \right) f_p. \end{aligned} \quad (2)$$

The wave frequency in the rotating frame scales as  $f_* \propto N_L^{1/2} L_p^{-1}$ , with  $f_* = 1.13$  MHz for our plasmas, substantially below the plasma frequency  $f_p \sim 35$  MHz. (Note that proper interpretation of theory [18] gives  $j_{m_\theta-1, m_r}$  rather than  $j_{m_\theta, m_r}$ .) At low amplitudes, these modes are *overdamped*, with Landau damping giving  $\gamma_L \sim 2.4 f_*$ , following from  $v_{ph} = 2L_p f_* \sim 2.6\bar{v}$ .

Despite the strong linear damping, application of resonant oscillating wall voltages does excite either mode to a large amplitude, long-lived BGK state. Figure 2 shows the (upper-mode) eigenfunction amplitude  $\delta n(r)$  obtained immediately after excitation; the eigenfunction agrees closely with the

$$\delta n(r) \propto n(r) J_1(j_{0,1} r / R_p) \quad (3)$$

prediction of linear theory.

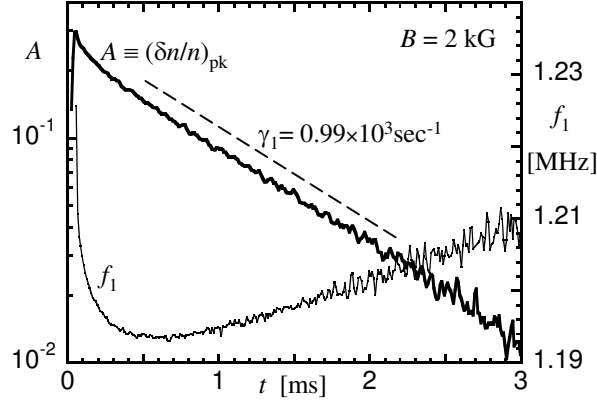


**FIGURE 3.** Peak mode amplitude and frequency vs. time after excitation.

Figure 3 shows the time evolution of the mode amplitude  $A \equiv (\delta n/n)_{\text{pk}}$  and frequency  $f_1(t)$ , obtained by fitting a local sinusoid to the waveform  $A_w(t)$  received on a wall sector. The  $m_\theta = 1$  BGK mode damps essentially exponentially over  $1\frac{1}{2}$  decades, at a rate  $\gamma_1 \sim 0.99 \times 10^3 \text{ sec}^{-1}$ ; this will be shown to be TPM collisional damping. At small amplitude the wave damps much more rapidly.

The mode frequency shows an ill-understood 4% decrease during excitation and the first 200 wave cycles (200  $\mu\text{sec}$ ); then shows a characteristic logarithmic increase [a retreat back to  $f_1(0)$ ] as the amplitude decreases. This latter evolution is well-approximated by  $f(A) = f_0 [1 - \alpha \ln(1 + \beta A)]$ . We note that the same amplitude dependence is observed with larger  $\alpha$  for  $m_\theta = 0$ ,  $m_r = 1$  BGK states [12, 13] apparently not mitigated by  $\pm\theta$  or radial layer cancellations.

Several experimental manipulations help to characterize the BGK mode. First, the damping can be greatly and immediately enhanced (5–10 $\times$ ) by lowering the end confinement voltage  $V_c$ , thereby allowing electrons in the wave-trapped phase-space vortex to escape. The wave then continually accelerates electrons to high velocities where they escape, and the wave damps rapidly.

This wave-trapped vortex is a “flat” component of  $F(E_z)$  comprising about 0.5% of the electrons. To obtain  $F(E_z)$ , the number of escaping electrons  $\Delta N_e$  is measured as the dump-end confinement voltage is ramped from  $V_c = -100\text{V}$  to  $V_c = -30\text{V}$  (close to the plasma potential  $\phi_p$ ) in a time of 100 $\mu\text{s}$ , as shown in Fig. 4. One expects  $\Delta N_e = \int dr \int_{\phi_p(r)-V_c}^{\infty} d\varepsilon F(\varepsilon)$ . Before (and long after) the wave is excited, the observed  $\Delta N_e(V_c)$  is exponential, reflecting a Maxwellian tail with  $T \sim 1 \text{ eV}$  [19]. During the BGK wave, the  $\Delta N_e(V_c)$  data reflects this Maxwellian distribution *plus* a flat distribution extending from  $\varepsilon = 0$  to  $\varepsilon_{\text{max}} = 17T$ . This maximum wave-trapping energy determines the wave potential  $\delta\phi_{\text{trap}} \sim 1.8V = 1.8T/e$ . This corresponds well to the wave potential  $\delta\phi^{\text{pk}} \sim 2.4 \text{ Volts}$  calculated from Poisson’s equation using the peak amplitude of Fig. 3, noting that the quantitative effects of  $r$ -averaging have not been calculated.

To destroy this wave-trapped vortex (forming the BGK state) it is sufficient to temporarily slightly open a confinement gate by lowering the confinement voltage  $V_c$ . Figure 5 shows that temporarily lowering down to  $V_c = -50\text{V}$  (which corresponds to the

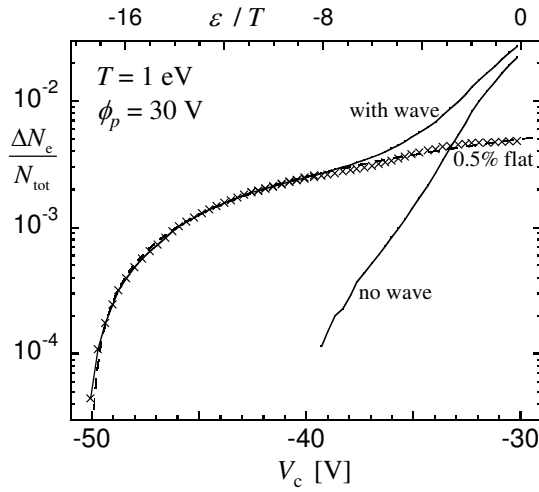


**FIGURE 4.** Fraction of escaped electrons  $\Delta N_e$  vs. confinement potential  $V_c$  (or thermal energy  $\varepsilon/T$ ) with and without wave. The measured difference (crosses) closely corresponds to a 0.5% flat fraction extending to  $17T$  (dashed).

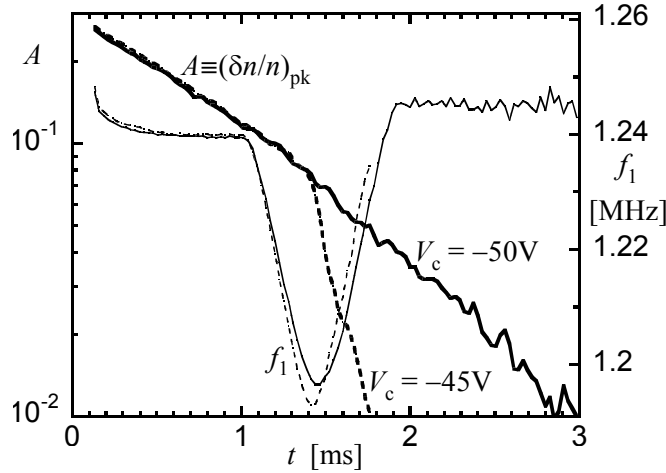


**FIGURE 5.** Enhanced damping of the  $m_\theta = 1$  BGK mode by partial ejection of the wave-trapped vortex. Solid lines correspond to confinement voltage lowered to  $V_c = -50V$ , and the dashed lines to  $V_c = -45V$ . The reversible dip in frequency  $f_1$  is due to changes in plasma parameters caused by  $V_c(t)$ .

most extreme high energy extent of the wave-trapped vortex at Fig. 4) just barely affects the damping rate. On the other hand, temporarily opening the confinement gate a little bit more down to  $V_c = -45V$  increases the damping rate dramatically. Due to fast trapping oscillations, a significant fraction of the vortex escapes the confinement region, and the BGK state shows a rapid decay. At this  $V_c$ , there would be negligible losses from the unperturbed Maxwellian distribution.

A second experimental technique demonstrates that other modes can enhance the ripple-separatrix crossings and thereby enhance the  $m_\theta = 1$  BGK mode damping. For

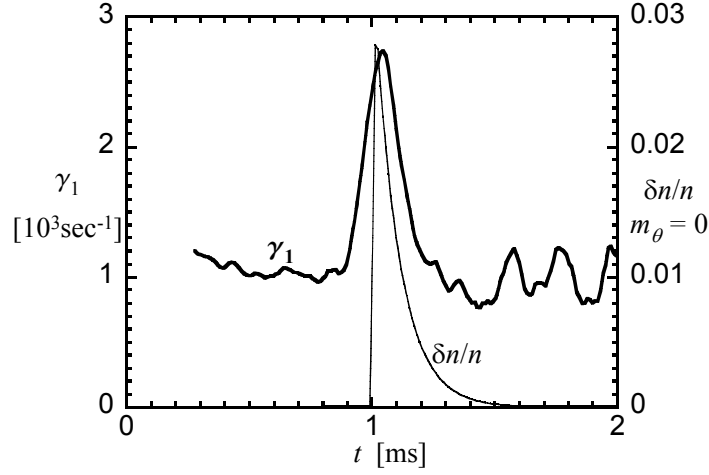


**FIGURE 6.** Enhanced damping  $\gamma_1$  of the  $m_\theta = 1$  BGK mode caused by excitation of an axisymmetric ( $m_\theta = 0$ ) TG mode at  $t = 1$  ms. Here, the bold line is  $\gamma_1(t)$ , and the light line is  $\delta n(t)/n$  of the strongly damped  $m_\theta = 0$  TG mode. The plotted  $\gamma_1(t)$  includes artificial broadening due to time averaging for noise reduction.

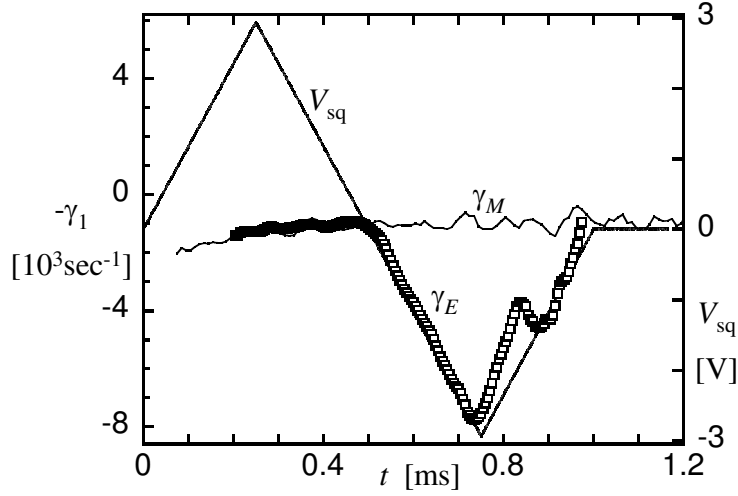


**FIGURE 7.** Enhanced damping  $\gamma_E$  induced by the negative portion of a ramped wall voltage  $V_{sq}$ ; the  $\gamma_M$  measurement is for  $V_{sq} = 0$ .

example, excitation of the  $m_\theta = 0$ ,  $m_z = 1$ ,  $m_r = 1$  (“sloshing”) Trivelpiece-Gould mode to a moderate amplitude causes a damping increment  $\Delta\gamma_1$  which is proportional to the  $m_\theta = 0$  excitation amplitude. Figure 6 shows a temporary increase in  $\gamma_1$  due to a short-lived TG mode excitation. The TG mode causes potential variations on  $\pm z$  ends of the ripple trapping barrier(s), resulting in enhanced ripple-separatrix crossings and enhanced  $m_\theta = 1$  mode damping. This technique has been used extensively to characterize TPM mode damping and particle transport [4], and even to diagnose  $F(E_z, r)$  at the separatrix velocity  $v_s(r)$  [20].

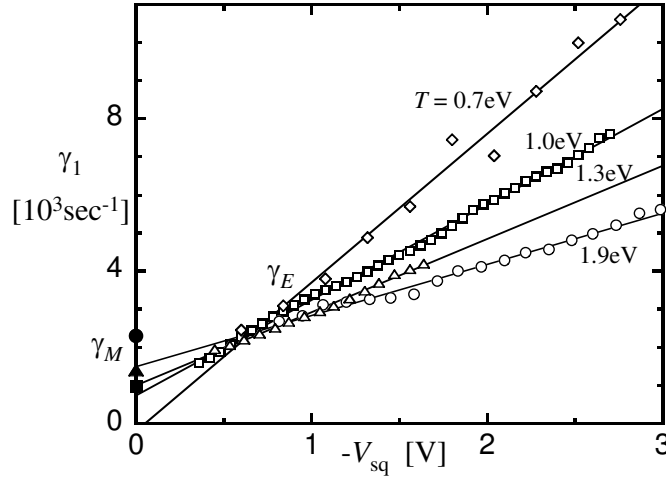


**FIGURE 8.** Damping rate  $\gamma_E$  vs. squeeze voltage  $V_{sq}$  at various plasma temperatures. Solid symbols show damping rate  $\gamma_M$  at  $V_{sq} = 0$ .

Third and most incisive, the BGK state damping can be enhanced by application of near-DC “squeeze” voltages on the mid-plane cylinder: these create *electric* trapping barriers in addition to the always-present *magnetic* ripple trapping barriers. Moreover, the effect of the squeeze is observed “instantaneously,” since the wave amplitude  $A(t)$  is obtained from a sinusoidal fit to  $A_w(t)$  over a time of only a few wave cycles.

Figure 7 shows the instantaneous effect on damping rate  $\gamma_1$  from a positive/negative ramped squeeze voltage applied to the mid-plane cylinder. Note that this is at the same axial position as the predominant magnetic ripple (mirror) of  $\delta B/B \sim 10^{-3}$ , and is at the node of the standing plasma wave. The positive squeeze has little effect, whereas the negative voltage creates an electric trapping barrier which gives strong TPM damping from the electric trapping barrier.

We interpret the observed damping as due to separate electric and magnetic trapping barriers, i.e.,  $\gamma_1 = \gamma_E + \gamma_M$ . The electric-TPM component  $\gamma_E$  is proportional to the strength of the electric trapping barrier, as shown in Fig. 8. Here, the instantaneous damping rate  $\gamma_1$  is plotted versus the instantaneous (negative) squeeze voltage  $V_{sq}$  for 4 different plasmas at varying temperatures. That is, the data at each  $T$  is obtained from  $\gamma_E(t)$  as in Fig. 7. The different temperatures are obtained by pre-heating with end-confinement-voltage variations near the electron bounce frequency of  $f_b \sim 1$  MHz.

For  $V_{sq} = 0$ , a (more accurate) damping rate is obtained over longer times, and this is interpreted as  $\gamma_M$  due to the inherent magnetic ripple. Prior experiments on cross-field transport and diocotron mode damping clearly isolated the magnetic ripple effects [2, 3, 4]; here, the requirement of 2 sectorized cylinders precludes removal of the ripple.

The temperature dependencies of  $\gamma_E$  and  $\gamma_M$  differ markedly. The observations suggest  $\gamma_E \propto eV_{sq}/T$ , which probably reflects a dependence on the number of electric-trapped particles, i.e.,  $\gamma_E \propto N_{tr}/N_{tot}$ . This dependence has been observed in prior TPM experiments on damping and transport with electric trapping [3, 4]. In contrast, a weakly positive dependence is obtained for  $\gamma_M(T)$ , but this has not been interpreted theoretic-

cally.

This TPM damping shows essentially no dependence on  $B$ , verified over the range  $1 \leq B \leq 15$  kG where  $f_R/f_* \ll 1$ . In this regime, the TPM damping rates are essentially equal for the upper and lower BGK modes.

The measured TPM damping rates are approximately  $50\times$  larger than a collisional Zakharov-Karpman estimate, which gives  $\gamma_{\text{ZK}} \sim 20 \text{sec}^{-1}$ . This is consistent with the  $80\times$  difference between  $\gamma_{\text{ZK}} \propto (v/f_*)^1 \sim 1.4 \cdot 10^{-4}$  and the (presumed)  $\gamma_{\text{TPM}} \propto (v/f_*)^{1/2} \sim 1.2 \cdot 10^{-2}$ . However, as yet this  $(v/f_*)^{1/2}$  scaling of TPM damping has been obtained theoretically only for “trapped-particle diocotron” modes [21], and substantial questions remain as to distribution function discontinuities, dissipation of equilibrium currents, and radial particle transport. Thus, the scaling remains uncertain.

TPM effects may contribute to the “rotating wall” technique for plasma manipulation and steady-state confinement, in at least some of the regimes where it has been applied [22, 23]. This is because TPM damping of  $m_\theta \neq 0$  modes necessarily couples wave angular momentum into the plasma particles, and causes radial transport of particles.

In conclusion, these experiments demonstrate that weak ripples in magnetic or electric confinement fields can produce dominant damping effects for non-axisymmetric plasma waves. These trapped-particle-mediated damping effects are particularly important in large-amplitude BGK states, where conventional collisional damping is much weaker.

## ACKNOWLEDGMENTS

This work was supported by National Science Foundation Grant No. PHY0354979.

## REFERENCES

1. A.A. Kabantsev, C.F. Driscoll, T.J. Hilsabeck, T.M. O’Neil, and J.H. Yu, *Phys. Rev. Lett.* **87**, 225002 (2001).
2. C.F. Driscoll, A.A. Kabantsev, T.J. Hilsabeck, and T.M. O’Neil, “Trapped-Particle-Mediated Damping and Transport,” in *Non-Neutral Plasma Physics V*, edited by M. Schauer et al., AIP Conf. Proc. **692**, American Institute of Physics, Melville, NY, 2003, pp. 3-14; A.A. Kabantsev and C.F. Driscoll, *Bull. Amer. Phys. Soc.* **49**, 318 (2004).
3. A.A. Kabantsev and C.F. Driscoll, *Phys. Rev. Lett.* **89**, 245001 (2002).
4. A.A. Kabantsev, J.H. Yu, R.B. Lynch, and C.F. Driscoll, *Phys. Plasmas* **10**, 1628 (2003).
5. M.N. Rosenbluth, D.W. Ross, and D.P. Kostomarov, *Nucl. Fusion* **12**, 3 (1972).
6. J. Slough, G.A. Navratil, and A.K. Sen, *Phys. Rev. Lett.* **47**, 1057 (1981).
7. G.A. Navratil, A.K. Sen, and J. Slough, *Phys. Fluids* **26**, 1044 (1983).
8. H.R. Wilson, J.W. Connor, R.J. Hastie, and C.C. Hegna, *Phys. Plasmas* **3**, 248 (1996).
9. C.D. Beidler, W.N.G. Hitchon, W.I. van Rij, S.P. Hirshman, and J.L. Shohet, *Phys. Rev. Lett.* **58**, 1745 (1987).
10. M. Bernstein, J.M. Greene, and M.D. Kruskal, *Phys. Rev.* **108**, 546 (1957).
11. J.R. Danielson, F. Anderegg, and C.F. Driscoll, *Phys. Rev. Lett.* **92**, 245003 (2004).
12. J.D. Moody and C.F. Driscoll, *Phys. Plasmas* **2**, 4482 (1995).
13. W. Bertsche and J. Fajans, *Phys. Rev. Lett.* **91**, 265003 (2003).
14. F. Valentini, T.M. O’Neil and D.H.E. Dubin, “Excitation and Decay of Electron Acoustic Waves,” this proceedings.
15. V.E. Zakharov and V.I. Karpman, *Sov. Phys. JETP* **16**, 351 (1963).
16. R.L. Sperl, *Phys. Fluids* **21**, 514 (1978).

17. I.D. Kaganovich, *Phys. Rev. Lett.* **82**, 327 (1999).
18. S.A. Prasad and T.M. O'Neil, *Phys. Fluids* **26**, 665 (1983); A.A. Kabantsev, "TG Mode Frequency Correction," <http://sdphA2.ucsd.edu>.
19. A.W. Hyatt, C.F. Driscoll, and J.H. Malmberg, *Phys. Rev. Lett.* **59**, 2975 (1987).
20. A.A. Kabantsev and C.F. Driscoll, *Rev. Sci. Instrum.* **74**, 1925 (2003).
21. T.J. Hilsabeck, A.A. Kabantsev, C.F. Driscoll, and T.M. O'Neil, *Phys. Rev. Lett.* **90**, 245002 (2003).
22. F. Anderegg, E.M. Hollmann, and C.F. Driscoll, *Phys. Rev. Lett.* **81**, 4875 (1998); E.M. Hollmann, F. Anderegg, and C.F. Driscoll, *Phys. Plasmas* **7**, 2775 (2000).
23. J.R. Danielson and C.M. Surko, *Phys. Rev. Lett.* **94**, 0305001 (2005).